# Metal−Metal Bonding in $d^1d^1$ and $d^2d^2$ Bioctahedral Dimer Systems: A Density Functional Study of Face-Shared $M_2X_9^{3-}$ (M = Ti, Zr, Hf, V, Nb, Ta) Complexes

**Robert Stranger,* John E. McGrady, and Timothy Lovell**

Department of Chemistry, The Faculties, The Australian National University, Canberra, ACT 0200, Australia

*Received December 2, 1997*

Density functional theory is used to investigate the electronic and geometric structures and periodic trends in metal−metal bonding of $d^1d^1$ and $d^2d^2$ face-shared $M_2X_9^{3-}$ dimers of Ti, Zr, Hf ($d^1d^1$) and V, Nb, Ta ($d^2d^2$). For these systems three distinct coupling modes can be recognized, depending on the occupation of the trigonal $t_{2g}(a_1 + e)$ single-ion orbitals, which determine the ground-state geometry and extent of metal−metal bonding. For $Ti_2Cl_9^{3-}$, the $[a_1 \times a_1]$ broken-symmetry optimized structure, corresponding to significant delocalization of the metal-based $\sigma$ electrons, nicely rationalizes the strong antiferromagnetic coupling reported for $Cs_3Ti_2Cl_9$. The ground-state geometries for $Zr_2Cl_9^{3-}$ and $Hf_2Cl_9^{3-}$ correspond to complete delocalization of the metal-based electrons in a metal−metal $\sigma$ bond. For $V_2Cl_9^{3-}$, the global minimum is found to be the ferromagnetic $[a_1e \times e^2]$ spin-quintet state giving rise to a long V−V separation, consistent with the known structure and reported weak ferromagnetic behavior of $Cs_3V_2Cl_9$. For $Nb_2X_9^{3-}$ (X = Cl, Br, I) and $Ta_2Cl_9^{3-}$, the $[a_1e \times a_1e]$ spin-triplet state, where complete delocalization of the $\sigma$ and $\delta_\pi$ electrons occur in a metal−metal double bond, is found to be the global minimum and consequently relatively short internuclear distances result, again, in good agreement with experiment. The periodic trends in metal−metal bonding in these and the isovalent $d^3d^3$ complexes can be rationalized in terms of the energetic contributions of orbital overlap ($\Delta E_{ovlp}$) and spin polarization ($\Delta E_{spe}$), the difference $\Delta E_{spe} - \Delta E_{ovlp}$ determining the tendency of the metal-based electrons to delocalize in the dimer. For $d^1d^1$ systems, $\Delta E_{ovlp}$ is always greater than $\Delta E_{spe}$ and therefore delocalized ground states result for all complexes of the titanium triad. Across the first transition series, the dramatic increase in $\Delta E_{spe}$ dominates $\Delta E_{ovlp}$ and therefore $V_2Cl_9^{3-}$ and $Cr_2Cl_9^{3-}$ have localized ground states. For the second and third transition series, the much larger $\Delta E_{ovlp}$ term ensures that all these complexes remain delocalized.

## Introduction

The calculation of the electronic structure of open-shell bimetallic systems, particularly those that exhibit magnetic interactions or bonding between metal centers, remains a challenging area of study due to the need to take proper account of electron correlation.[1] For symmetric dimer systems, the presence of symmetry elements connecting the two metal centers forces complete electron delocalization, leading to a poor description of the metal−metal bond for weakly coupled systems. To describe correctly this weakly coupled limit, it is necessary for the metal centers to behave independently, thus enabling the magnetic electrons to localize on one center or the other. This may be achieved through use of the broken-symmetry method,[2] developed by Noodleman and co-workers, which has been successfully applied in the treatment of a wide variety of dinuclear and polynuclear transition-metal-based systems, including magnetically coupled centers in metalloproteins.[3]

In the broken-symmetry method, the symmetry elements connecting the two halves of the dimer are removed (symmetry-breaking) and an asymmetry in the unpaired spin density is introduced at the two metal centers in order to facilitate localization of the magnetic electrons. This approach is particularly attractive as it allows the two metal centers to be treated as distinct weakly interacting subunits on which the magnetic electrons involved in the coupling are free to localize. It should be emphasized that the broken-symmetry approach does not force the magnetic electrons to localize, it merely permits such a situation if the delocalized alternative is less stable. In the limit of strong metal−metal bonding however, the broken-symmetry solution is identical to that obtained from a full-symmetry calculation where complete delocalization of the magnetic electrons is necessarily imposed. The broken-symmetry approach therefore encompasses both the weak antiferromagnetically coupled (localized) and strong metal−metal bonded (delocalized) limits as well as a continuum of intermediate situations, making it an ideal tool to study periodic trends in metal−metal bonding.

(1) (a) Bénard, M. *Quantum Chemistry*: *Basic Aspects, Actual Trends*; Carlo, R. Ed.; Elsevier: Amsterdam, 1989. (b) Ziegler, T. *Chem. Rev.* **1991**, *91*, 651.

(2) (a) Noodleman, L.; Norman, J. G., Jr. *J. Chem. Phys.* **1979**, *70*, 4903. (b) Noodleman, L. *J. Chem. Phys.* **1981**, *74*, 5737.

(3) (a) Aizman, A.; Case, D. A. *J. Am. Chem. Soc.* **1982**, *104*, 3269. (b) Noodleman, L.; Baerends, E. J. *J. Am. Chem. Soc.* **1984**, *106*, 2316. (c) Bencini, A. Gatteschi, D. *J. Am. Chem. Soc.* **1986**, *108*, 5763. (d) Ross, P. K.; Solomon, E. I. *J. Am. Chem. Soc.* **1991**, *113*, 3246. (e) Noodleman, L.; Case, D. A. *Adv. Inorg. Chem.* **1992**, *38*, 423. (f) Mouesca, J.-M.; Chen, J. L.; Noodleman, L.; Bashford, D.; Case, D. A. *J. Am. Chem. Soc.* **1994**, *116*, 11898. (g) Medley, G. A.; Stranger, R. *Inorg. Chem.* **1994**, *33*, 3976. (h) Brown, C. A.; Remar, G. J.; Musselman, R. L.; Solomon, E. I. *Inorg. Chem.* **1995**, *34*, 688. (i) Zhao, X. G.; Richardson, W. H.; Chen, J.-L.; Li, J.; Noodleman, L. *Inorg. Chem.* **1997**, *36*, 1198. (j) McGrady, J. E.; Stranger, R. *J. Am. Chem. Soc.* **1997**, *119*, 8512.1

10.1021/ic971511y CCC: $15.00 
Published on Web 12/01/1998

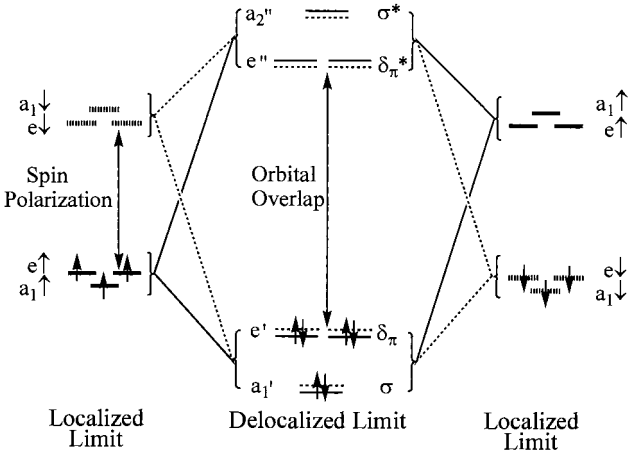


**Figure 1.** Representation of the broken-symmetry state of $\{d^3d^3\}$ $M_2Cl_9$ dimers in both localized and delocalized limits. Orbitals are labeled according to the representations of the $C_{3v}$ point group in the localized case and the $D_{3h}$ point group in the delocalized case.

In a previous communication we discussed the importance of symmetry-breaking in the calculation of metal−metal separations in the face-shared $d^3d^3$ bioctahedral dimers $[M_2Cl_9]^{3-}$ (M = Cr, Mo, W) using density functional theory (DFT).[4] More recently we have described in detail the nature of the broken-symmetry state in these and the isoelectronic $d^3d^3$ metal nonachloride $[M_2Cl_9]^-$ (M = Mn, Tc, Re) and edge-shared decachloride $[M_2Cl_{10}]^{4-}$ (M = Cr, Mo, W) complexes as well as the mixed-metal series $[MM'Cl_9]^{3-}$ ($M \neq M' =$ Cr, Mo, W) and $[MM'Cl_9]^-$ ($M \neq M' =$ Mn, Tc, Re).[5] The qualitative features of the interaction between the metal-based orbitals in these complexes are shown in Figure 1. The local trigonal $C_{3v}$ symmetry at each metal center splits the octahedral $t_{2g}$ set into a nondegenerate $a_1$ orbital having $\sigma$ symmetry with respect to the metal−metal axis and a doubly degenerate e set having mixed $\delta$ and $\pi$ (denoted $\delta_\pi$) symmetry. In the weakly coupled limit, these magnetic orbitals remain localized on their respective metal centers and the metal−metal interaction is only a small perturbation on the energy levels of the two isolated single ions. For the single-ion $d^3$ configuration, each of these orbitals is singly occupied with the electron spins parallel. As a result of this spin polarization, the majority-spin, occupied metal-based orbitals lie significantly lower in energy than their minority spin, vacant, counterparts (Figure 1, localized limit). As the metal−metal interaction increases, the magnetic orbitals become progressively more delocalized over both centers resulting in $\sigma(a_1')$ and $\delta_\pi(e')$ bonding and $\sigma^*(a_2'')$ and $\delta_\pi^*(e'')$ antibonding combinations for $D_{3h}$ symmetry. The delocalization of the electrons occupying these orbitals lowers the spin density at each metal center, thereby reducing the spin polarization splitting, while an increase in the orbital overlap results in significant splitting between bonding and antibonding counterparts (Figure 1, delocalized limit). Thus, the splittings within the energy level scheme shown in Figure 1 arise from two very different sources, depending on the extent of delocalization. In the weakly coupled limit, spin polarization is responsible for the separation between the occupied and vacant orbitals, whereas in the delocalized limit, orbital overlap causes a splitting between bonding and antibonding pairs resulting in a net metal−metal triple bond for the $d^3d^3$ configuration. Between these localized and delocalized limits lies a continuum of situations in which the metal-based electrons are partially delocalized over the two metal centers.

Without making any assumptions regarding the extent of delocalization of the metal-based orbitals, and hence their bonding or antibonding character, the broken-symmetry state for a $d^3d^3$ complex can always be defined by the antiferromagnetic configuration $(a_1\uparrow)^1(a_1\downarrow)^1(e\uparrow)^2(e\downarrow)^2(e\uparrow)^0(e\downarrow)^0(a_1\uparrow)^0(a_1\downarrow)^0$ where the magnetic electrons on adjacent centers have opposite spin. For the broken-symmetry state, the orbitals are labeled according to the representations of the $C_{3v}$ point group to emphasize that there is no symmetry-imposed barrier to localization. The simplest way to determine which subsets ($\sigma$ or $\delta_\pi$) of electrons are delocalized in the broken-symmetry state at a given metal−metal separation is to examine the three associated spin states, $S = 3$, 2, and 0, each of which can be expressed as a single determinantal wave function. For these states, the orbitals are labeled according to the full molecular symmetry ($D_{3h}$) because in each case the electrons are found to be fully delocalized, even in the absence of imposed symmetry elements linking the two metal centers, thus yielding eigenstates equivalent to full $D_{3h}$ electronic symmetry. The $S = 3$ state is defined by the $(a_1'\uparrow)^1(a_1'\downarrow)^0(e'\uparrow)^2(e'\downarrow)^0(e''\uparrow)^2(e''\downarrow)^0(a_2''\uparrow)^1(a_2''\downarrow)^0$ configuration, where all metal-based electrons are aligned in parallel (ferromagnetically coupled). Similarly, $S = 2$ is defined by $(a_1'\uparrow)^1(a_1'\downarrow)^1(e'\uparrow)^2(e'\downarrow)^0(e''\uparrow)^2(e''\downarrow)^0(a_2''\uparrow)^0(a_2''\downarrow)^0$, where only the $\delta_\pi$ electrons are aligned parallel, the $\sigma$ subset remaining antiferromagnetically coupled. Finally, the $S = 0$ state is defined by the configuration $(a_1'\uparrow)^1(a_1'\downarrow)^1(e'\uparrow)^2(e'\downarrow)^2(e''\uparrow)^0(e''\downarrow)^0(a_2''\uparrow)^0(a_2''\downarrow)^0$.

The connection between the $S = 3$, 2, and 0 associated states and the broken-symmetry state can be made by noting that when antiferromagnetic coupling within a subset of electrons is weak, then the corresponding ferromagnetic associated state, where the weakly coupled electrons are now aligned in parallel, must lie close in energy. Thus, when all electrons are weakly coupled, the $S = 3$ state will lie close to the broken-symmetry state, whereas when only the $\delta_\pi$ subset is weakly coupled, the $S = 2$ state will lie closest. Finally, when all electrons are completely delocalized, the broken-symmetry state is identical to $S = 0$ in which full delocalization is enforced. Except in this fully delocalized limit, the energy of the true antiferromagnetic $S = 0$ state cannot be calculated directly, due to its multideterminantal nature, but can be obtained indirectly from the energies of the broken-symmetry state and associated ferromagnetic state using spin-projection techniques.[2b,3e] However, this procedure is only valid in the limit of weak coupling between the metal centers and we have recently shown that over the regions of the broken-symmetry potential energy curve where it is valid to perform spin projection, the antiferromagnetic $S = 0$ state invariably lies close in energy to the broken-symmetry state and therefore spin projection is not necessary.[5a]

An important feature of the above discussion is that each coupling scheme is only valid over a limited range of $r$M−M corresponding to where the potential energy curve for the appropriate associated state lies parallel and close to the broken-symmetry curve. Thus, the nature of the metal−metal bonding in the broken-symmetry state in these complexes is ultimately determined by which associated state, and therefore which region of the broken-symmetry potential energy curve, lies lowest in energy. In Figure 2a, the $S = 0$ state lies lowest, and the global minimum for the broken-symmetry state lies at short metal−metal separations due to the complete delocalization of the $\sigma$ and $\delta_\pi$ electrons in metal−metal bonds. In Figure 2c, the $S =$

(4) Lovell, T.; McGrady, J. E.; Stranger, R.; Macgregor, S. A. *Inorg. Chem.* **1996**, *35*, 3079.

(5) (a) McGrady, J. E.; Stranger, R.; Lovell, T. *J. Phys. Chem.* **1997**, *101A*, 6265. (b) McGrady, J. E.; Stranger, R.; Lovell, T. *Inorg. Chem.* **1997**, *36*, 3242. (c) McGrady, J. E.; Stranger, R.; Lovell, T. *Inorg. Chem.* **1998**, *37*, 3802.

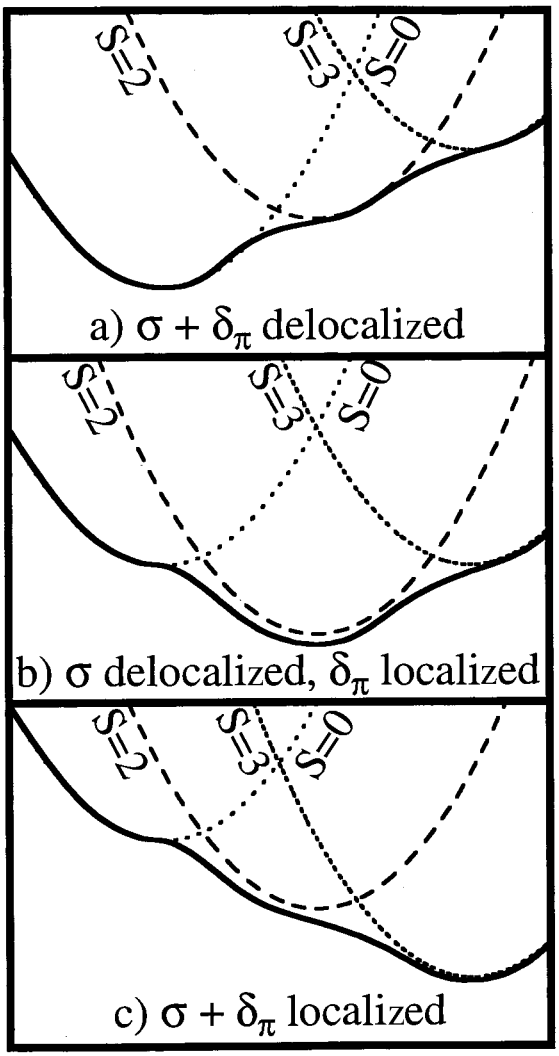


**Figure 2.** Schematic representation of the potential energy curves for the broken-symmetry and $S = 0$, 2, and 3 associated spin states for $M_2Cl_9$ complexes with the $\{d^3d^3\}$ configuration.

3 state is the most stable and the broken-symmetry optimized separation is large due to all metal-based electrons being weakly coupled. Finally, in Figure 2b the $S = 2$ state is lowest and an intermediate broken-symmetry optimized separation results as a consequence of the $\delta_\pi$ electrons being weakly coupled while the $\sigma$ electrons are effectively delocalized in a metal−metal $\sigma$ bond.

Having established the main features of the broken-symmetry potential energy curves in the $d^3d^3$ systems, where the $t_{2g}$ orbitals are exactly half-filled, we now extend the analysis to the $d^1d^1$ and $d^2d^2$ systems, where the combination of the trigonal field and orbital degeneracy gives rise to more than one possible choice for the single-ion ground-state configuration. For instance, in $d^1d^1$ complexes, the single-ion configuration may correspond to an electron in either the $a_1$ or e trigonal orbitals. In the dinuclear complex, the former configuration can give rise to a metal−metal $\sigma$ bond whereas the latter configuration can only result in metal−metal $\delta_\pi$ bonding. Thus, the type and extent of metal−metal interaction, and therefore the predicted ground state geometry, may be strongly dependent on the chosen single-ion configuration. We now examine potential energy curves for the broken-symmetry and other spin states of the $d^1d^1$ systems, $Ti_2Cl_9^{3-}$, $Zr_2Cl_9^{3-}$, $Hf_2Cl_9^{3-}$, and their isovalent $d^2d^2$ analogues, $V_2Cl_9^{3-}$, $Nb_2Cl_9^{3-}$, and $Ta_2Cl_9^{3-}$, and compare the results with the previously reported data on the $d^3d^3$ complexes of the chromium triad. In so doing, we aim to delineate the various factors involved in controlling the strength of metal−metal interactions, and draw conclusions regarding periodic trends in metal−metal bonding.

## Computational Details

All approximate density functional calculations reported in this work were performed on IBM RISC6000 or Sun UltraSparc 140/170 workstations using the Amsterdam Density Functional (ADF) program version 2.3 developed by Baerends et al.[6] A double-$\zeta$ Slater type orbital basis set extended with a single d-polarization function was used to describe chlorine, bromine and iodine atoms, while all metals atoms were modeled with a triple-$\zeta$ basis set. Electrons in orbitals up to and including 2p {Cl}, 3p {Ti, V}, 3d {Br}, 4p {Zr, Nb}, 4d {I}, and 5p {Hf, Ta} were considered to be part of the core and treated in accordance with the frozen-core approximation. Geometry optimizations were performed using the gradient algorithm of Versluis and Ziegler.[7] Calculations on the $M_2X_9^{3-}$ dimers were performed in either a restricted or unrestricted manner using $D_{3h}$ and $C_{3v}$ symmetry for the full- and broken-symmetry calculations, respectively, while those on the monomeric $MX_6^{3-}$ complexes were performed using $O_h$ symmetry. For the broken-symmetry calculations, all symmetry elements connecting the two metal centers were removed and an initial asymmetry in spin density introduced using the "modifystartpotential" key. The LDA approximation was used, along with the local exchange-correlation potential of Vosko, Wilk, and Nusair.[8] Neither gradient nor quasi-relativistic corrections were considered as they have been shown to result in generally poorer agreement with the crystallographically determined structures than the LDA in isolation.[5a] The potential energy curves for the broken-symmetry and spin-singlet, -triplet, and -quintet states were generated by freezing the metal−metal separation, *r*M−M, at 0.1 Å intervals and optimizing all other independent structural parameters. With the exception of the broken-symmetry states, all other calculations were carried out using the full-symmetry ($D_{3h}$) of the dimers.

## Results and Discussion

In the following analysis, we focus primarily on the broken-symmetry (BS) and associated states which arise from antiferromagnetic and ferromagnetic coupling of the same subset ($\sigma + \delta_\pi$) of electrons on opposite metal centers, respectively. Accordingly, we do not attempt to calculate the energies of all possible states arising from the various $d^1d^1$ and $d^2d^2$ coupling modes since in general many of these states are multideterminantal in nature and as such not amenable to calculation using a single-determinant DFT approach. In some instances, namely where orbitally degenerate single-ion ground states are involved, the associated states will in fact correspond to a mixture of two or more multiplets arising from the same configuration.

**$d^1d^1$ Complexes.** From Figure 1, the magnetic electrons in a $d^1d^1$ complex can reside in either the trigonal $a_1$ or e single-ion orbitals, giving rise to three possible coupling modes between the two metal centers, denoted henceforth as $[a_1 \times a_1]$, $[e \times e]$, and $[a_1 \times e]$. Taking the $Ti_2Cl_9^{3-}$ system as a representative example, we examine each of these three coupling modes in turn, considering both the broken-symmetry and associated states as well as other states which arise as a consequence of the degeneracy of the trigonal e orbitals. The qualitative features of the potential energy curves for $Ti_2Cl_9^{3-}$ will then be used to rationalize bonding trends in the heavier congeners.

For the $[a_1 \times a_1]$ symmetric coupling mode, where an electron occupies the trigonal $a_1$ orbital on each metal center, the single-

(6) (a) Baerends, E. J.; Ellis D. E.; Ros, P. *Chem. Phys.* **1973**, *2*, 42. (b) Baerends, E. J.; Ros, P. *Int. J. Quantum Chem.* **1978**, *S12*, 169. (c) teVelde, G.; Baerends, E. J. *J. Comput. Phys.* **1992**, *99*, 84.
(7) Versluis, L.; Ziegler, T. J. *Chem. Phys.* **1988**, *88*, 322.
(8) Vosko, S. H.; Wilk, L.; Nusair, M. *Can. J. Phys.* **1980**, *58*, 1200.

**Scheme 1**

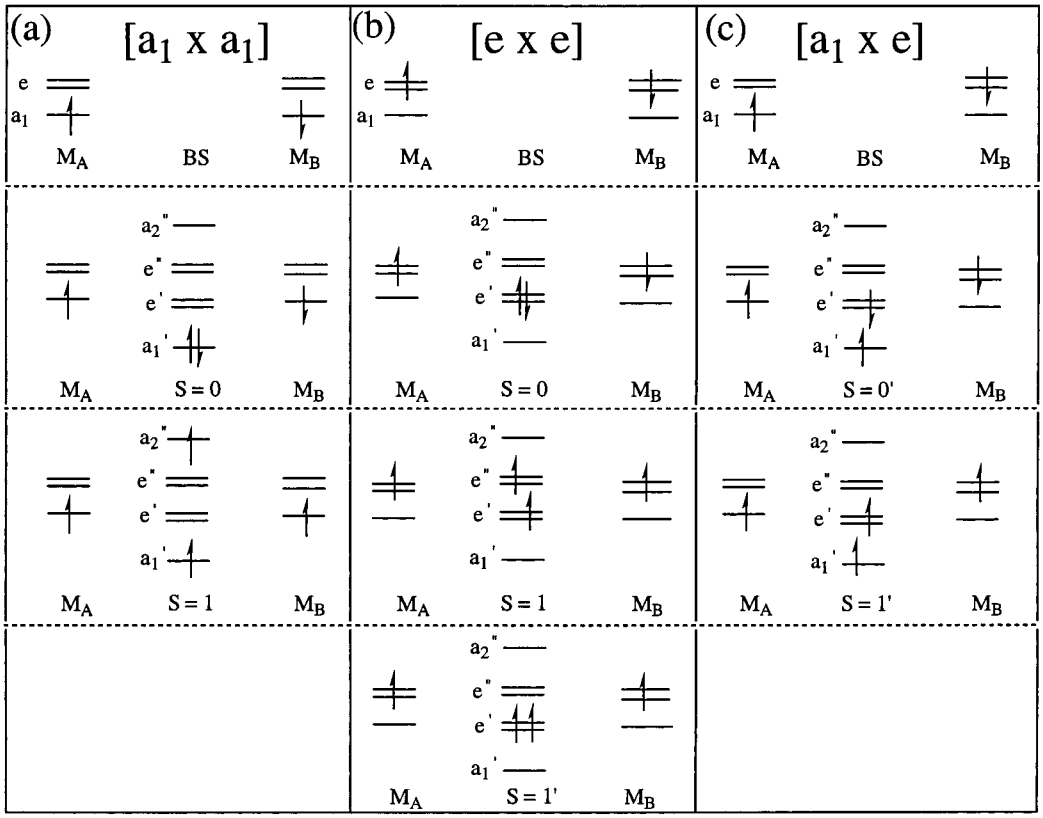


ion ground state corresponds to the orbitally nondegenerate $^2A_1$ level, and coupling between the two metal centers results in spin-singlet ($S = 0$) and spin-triplet ($S = 1$) dimer levels, $^1A_1' + {}^3A_2''$, in $D_{3h}$ symmetry. For this coupling scheme, the broken symmetry state is defined by the antiferromagnetic configuration $(a_1\uparrow)^1(a_1\downarrow)^1(e\uparrow)^0(e\downarrow)^0(e\uparrow)^0(e\downarrow)^0(a_1\uparrow)^0(a_1\downarrow)^0$, while the associated ferromagnetic spin-triplet state, $S = 1$, corresponds to the full-symmetry configuration $(a_1'\uparrow)^1(a_1'\downarrow)^0(e'\uparrow)^0(e'\downarrow)^0(e''\uparrow)^0(e''\downarrow)^0(a_2''\uparrow)^1(a_2''\downarrow)^0$ (Scheme 1a). The $S = 0$ associated state, corresponding to complete delocalization of the $\sigma$ subset of electrons occupying the single-ion $a_1$ orbitals, is defined by the $(a_1'\uparrow)^1(a_1'\downarrow)^1(e'\uparrow)^0(e'\downarrow)^0(e''\uparrow)^0(e''\downarrow)^0(a_2''\uparrow)^0(a_2''\downarrow)^0$ configuration. The energies and metal−metal separations of the minima in all three states are given in Table 1. The potential energy curves as a function of the metal−metal separation for all three states are shown in Figure 3a and can be interpreted in fashion similar to the $d^3d^3$ systems described previously. In the limit of weak antiferromagnetic coupling ($r$Ti−Ti > 3.4 Å), the curve for the $S = 1$ associated state, corresponding to ferromagnetic coupling of the $\sigma$ subset of electrons, lies parallel and close to the broken-symmetry curve. As the metal−metal separation is decreased, the stronger coupling between the metal-based electrons eventually leads to full delocalization of the metal-based electrons, at which point the broken-symmetry state converges with the $S = 0$ associated state ($r$Ti−Ti < 3.0 Å), where delocalization is enforced. In the intermediate region, the broken-symmetry potential energy curve makes a smooth transition between the $S = 1$ and $S = 0$ associated states. The position of the minimum in the broken-symmetry curve is therefore determined by the relative energies of the $S = 0$ and $S = 1$ associated states, which in this case is $S = 0 < S = 1$. The global minimum for the [$a_1 \times a_1$] coupling mode therefore corresponds to full delocalization of the metal-based electrons in a Ti−Ti $\sigma$ bond, and a relatively short metal−metal separation of 2.87 Å. The calculated net spin density for the broken-symmetry state, indicates that complete delocalization of the metal-based electrons in a Ti−Ti $\sigma$ bond occurs for $r$Ti−Ti < 3.0 Å.

**Table 1.** Optimized Metal−Metal Separations (Å) and Ground State Energies (eV) for the Various Spin States of $d^1d^1$ $M_2X_9$ Complexes

| | | [$a_1 \times a_1$] | | [e × e] | | [$a_1 \times$ e] | |
|---|---|---|---|---|---|---|---|
| | | M−M/Å | *E*/eV | M−M/Å | *E*/eV | M−M/Å | *E*/eV |
| $Ti_2Cl_9^{3-}$ | BS | 2.87 | −48.114 | 3.47 | −47.844 | 3.25 | −47.920 |
| | $S = 0$ | 2.87 | −48.114 | 3.40 | −47.140 | | |
| | $S = 1$ | 3.40 | −47.754 | 3.45 | −47.822 | | |
| | $S = 0'$ | | | | | 3.13 | −47.615 |
| | $S = 1'$ | | | 3.49 | −48.063 | 3.28 | −48.137 |
| $Zr_2Cl_9^{3-}$ | BS | 3.01 | −50.811 | 3.76 | −49.649 | 3.47 | −49.965 |
| | $S = 0$ | 3.01 | −50.811 | 3.60 | −49.009 | | |
| | $S = 1$ | 3.67 | −49.545 | 3.71 | −49.569 | | |
| | $S = 0'$ | | | | | 3.22 | −49.845 |
| | $S = 1'$ | | | 3.78 | −49.913 | 3.21 | −50.132 |
| $Hf_2Cl_9^{3-}$ | BS | 3.06 | −50.299 | 3.80 | −49.148 | 3.46 | −49.492 |
| | $S = 0$ | 3.06 | −50.299 | 3.63 | −48.524 | | |
| | $S = 1$ | 3.70 | −48.993 | 3.77 | −49.065 | | |
| | $S = 0'$ | | | | | 3.23 | −49.387 |
| | $S = 1'$ | | | 3.81 | −49.406 | 3.23 | −49.663 |
| $Ti_2Br_9^{3-}$ | BS | 2.99 | −43.279 | 3.61 | −43.104 | 3.45 | −43.150 |
| | $S = 0$ | 2.99 | −43.279 | 3.55 | −42.693 | | |
| | $S = 1$ | 3.59 | −43.036 | 3.61 | −43.089 | | |
| | $S = 0'$ | | | | | 3.26 | −43.120 |
| | $S = 1'$ | | | 3.67 | −43.298 | 3.45 | −43.358 |

In the other symmetric coupling mode [e × e], the metal-based electrons occupy the trigonal e orbitals on each center and the single-ion ground state corresponds to the orbitally degenerate $^2E$ level. Unlike the previous symmetric coupling mode, the orbital degeneracy results in several spin-singlet and -triplet dimer states arising from the coupling of the $\delta_\pi$ electrons.

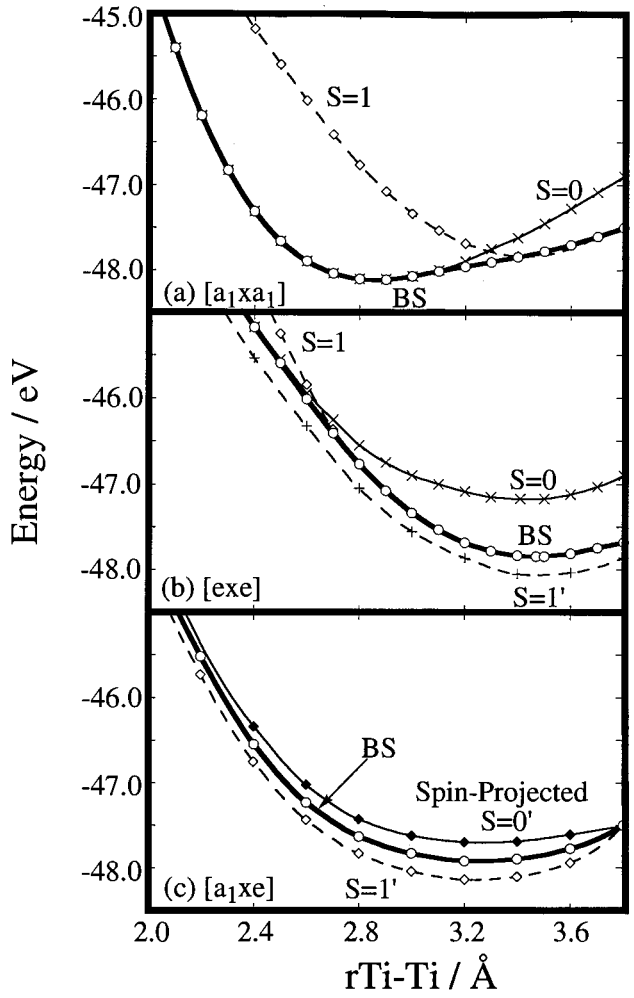


**Figure 3.** Potential energy curves for the broken-symmetry and $S = 0$, 1, and 1′ spin states for the $[a_1 \times a_1]$, $[e \times e]$, and $[a_1 \times e]$ coupling modes in $Ti_2Cl_9^{3-}$.

We will begin the analysis in analogous fashion to the $[a_1 \times a_1]$ case, by considering the antiferromagnetic broken-symmetry state and its associated spin states, before considering the additional spin states arising as a consequence of the degeneracy of the e orbital. By analogy with the previous example, the antiferromagnetic broken-symmetry state is defined by the configuration $(a_1\uparrow)^0(a_1\downarrow)^0(e\uparrow)^1(e\downarrow)^1(e\uparrow)^0(e\downarrow)^0(a_1\uparrow)^0(a_1\downarrow)^0$ and the $S = 0$ and ferromagnetic $S = 1$ associated states by the $(a_1'\uparrow)^0(a_1'\downarrow)^0(e'\uparrow)^1(e'\downarrow)^1(e''\uparrow)^0(e''\downarrow)^0(a_2''\uparrow)^0(a_2''\downarrow)^0$ and $(a_1'\uparrow)^0(a_1'\downarrow)^0(e'\uparrow)^1(e'\downarrow)^0(e''\uparrow)^1(e''\downarrow)^0(a_2''\uparrow)^0(a_2''\downarrow)^0$ configurations, respectively (see Scheme 1b). As a consequence of the orbital degeneracy however, both the singlet and triplet configurations involve more than one multiplet of the same spin. In fact, the singlet configuration is not even a pure spin state as it contributes to several states of different spin arising from the $(e')^2$ configuration, namely $^3A_2'$ ($M_S = 0$) + $^1A_1'$ + $^1E'$. In general, these states are multideterminantal and therefore cannot be calculated directly by DFT methods. However, significant progress can be made by using the sum method of Ziegler et al.[9] The underlying principle of this method is that the energy of a single determinant associated with a given configuration can, in general, be expressed as a weighted sum of energies of all multiplets arising from the same configuration. Thus, provided that the number of single determinants of different energy is the same as the number of multiplets of different energy, then it is possible, in principle, to determine the energies of all multiplets.

Using standard group theoretical methods,[10] the wave functions for the $^3A_2' + {}^1A_1' + {}^1E'$ multiplets can be written as

$$|^3A_2'\ M = +1> = |e'_a{}^+ e'_b{}^+|$$

$$|^3A_2'\ M = 0> = 1/\sqrt{2}\,[|e'_a{}^+ e'_b{}^-| - |e'_b{}^+ e'_a{}^-|]$$

$$|^1A_1'\ M = 0> = 1/\sqrt{2}\,[|e'_a{}^+ e'_a{}^-| + |e'_b{}^+ e'_b{}^-|]$$

$$|^1E'_a\ M = 0> = 1/\sqrt{2}\,[|e'_b{}^+ e'_b{}^-| - |e'_a{}^+ e'_a{}^-|]$$

$$|^1E'_b\ M = 0> = 1/\sqrt{2}[|e'_a{}^+ e'_b{}^-| + |e'_b{}^+ e'_a{}^-|]$$

where the subscripts a and b are used to distinguish the components of the doubly degenerate E state and e orbitals. Since the determinants $|e'_a{}^+e'_b{}^+|$, $|e'_a{}^+e'_b{}^-|$, and $|e'_a{}^+e'_a{}^-|$ are found to have different energies, it is relatively straightforward using the sum method[9] to express the energies of the above multiplets as a sum of the following single-determinant energies:

$$E(^3A_2') = E|e'_a{}^+ e'_b{}^+| \quad (1a)$$

$$E(^1E') = 2E|e'_a{}^+ e'_b{}^-| - E|e'_a{}^+ e'_b{}^+| \quad (1b)$$

$$E(^1A_1') = 2E|e'_a{}^+ e'_a{}^-| - 2E|e'_a{}^+ e'_b{}^-| + E|e'_a{}^+ e'_b{}^+| \quad (1c)$$

To determine the energies of the single-determinant configurations given in eqns 1a−c, it is necessary to distinguish between the two components of the doubly degenerate e′ representation. This can be achieved by carrying out the calculations in a lower symmetry point group which removes the orbital degeneracy, in this case $C_{2v}$ symmetry.

Similarly, the ferromagnetic triplet configuration $(a_1'\uparrow)^0(a_1'\downarrow)^0(e'\uparrow)^1(e'\downarrow)^0(e''\uparrow)^1(e''\downarrow)^0(a_2''\uparrow)^0(a_2''\downarrow)^0$ gives rise to $^3A_1'' + {}^3A_2'' + {}^3E''$ states in $D_{3h}$ symmetry. However, for these multiplets, only two single determinants are found which have different energies and consequently, it is not possible to express the multiplet energies as a sum of single-determinant energies. Fortunately, these states are not reasonable candidates for the global ground state in $Ti_2Cl_9^{3-}$, as will become apparent in the discussion to follow.

In addition to the $S = 0$ and $S = 1$ associated states described above, an additional spin triplet state, $^3A_2'$, defined by the full-symmetry configuration $(a_1'\uparrow)^0(a_1'\downarrow)^0(e'\uparrow)^2(e'\downarrow)^0(e''\uparrow)^0(e''\downarrow)^0(a_2''\uparrow)^0(a_2''\downarrow)^0$, arises as a consequence of the degeneracy of the e′ orbital. This configuration is related to the $S = 0$ configuration simply by flipping the spin of one electron (Scheme 1b). It is important to distinguish this delocalized state, denoted $S = 1'$, where the electrons are located in orthogonal components of the dimer e′ bonding orbital, from the associated $S = 1$ states described earlier where the electrons occupy both the e′ and e″ orbitals. To distinguish associated states from other spin states, the latter hereafter will be labeled with a prime.

Potential energy curves for the broken-symmetry state (BS), the $^1E'$ spin-singlet ($S = 0$) and average of the spin-triplet ($S = 1$) associated states, and the delocalized spin-triplet state ($S = 1'$) are shown in Figure 3b and the positions of their respective minima given in Table 1. The potential energy curve for $^1A_1'$ is not shown as it is found to lie at higher energy for all metal−

(9) Ziegler, T.; Rauk, A.; Baerands, E. J. *Theor. Chim. Acta* **1977**, *43*, 261.

(10) Griffith, J. S. *The Irreducible Tensor Method for Molecular Symmetry Groups;* Prentice Hall: Englewood Cliffs, NJ, 1962.

metal separations in the range 2 to 4 Å. In relation to the broken-symmetry and associated states, the qualitative features of the curves are rather similar to those shown in Figure 3a associated with the [$a_1 \times a_1$] coupling mode. At large metal−metal separations ($r$Ti−Ti > 2.7 Å), $S = 1$ lies close to the broken-symmetry curve, while at shorter separations ($r$Ti−Ti < 2.4 Å) the broken-symmetry and $S = 0$ states converge. There are, however, significant quantitative differences related to the weaker overlap of the $\delta_\pi$ orbitals on opposite centers. The energies of the associated states now decrease in the order $S = 1 < S = 0$, in direct contrast to the [$a_1 \times a_1$] mode, where the opposite ordering occurred. The minimum in the broken-symmetry state for the [e × e] mode therefore occurs at a long Ti−Ti separation of 3.47 Å, corresponding to almost complete localization of the metal-based electrons. Relatively short metal−metal separations of $r$Ti−Ti < 2.4 Å are required in order to bring about complete delocalization of the $\delta_\pi$ electrons and consequent formation of a Ti−Ti $\delta_\pi$ bond. Thus, we see that when the electrons are located in the $a_1$ single-ion orbitals, significant metal−metal $\sigma$ bonding arises, but when they are placed in their counterparts of e symmetry, the weaker $\delta_\pi$ overlap results in an effectively nonbonded situation.

For the [$a_1 \times a_1$] coupling mode the broken-symmetry state lies lowest in energy but this is not the case for the [e × e] mode. For the latter, Hund's rule dictates that the delocalized spin-triplet ($S = 1'$) state, $^3A_2'$, state should lie lower in energy than the corresponding singlet states, $^1A_1' + {}^1E'$, arising from the same configuration. Figure 3b confirms that the $S = 1'$ state does indeed lie at lower energy than, and parallel to, the broken-symmetry state at all points, with a minimum at very similar $r$Ti−Ti of 3.49 Å. Thus the global minimum in the [e × e] coupling mode corresponds to the triplet $S = 1'$ state rather than the broken-symmetry singlet state.

Finally, we consider the asymmetric coupling mode [$a_1 \times e$] where one electron occupies the $a_1$ orbital on one metal center while the second electron occupies the e orbital on the other. In this case, one metal has a $^2A_1$ ground state while the other has $^2E$ and coupling between them again results in spin-singlet and spin-triplet dimer levels. The [$a_1 \times e$] coupling mode is fundamentally different from the other two symmetric modes because antiferromagnetic coupling between the metal centers is precluded on the basis that the electrons are located in orthogonal orbitals. Consequently, ferromagnetic coupling dominates and there is no driving force for electron localization. We may define the broken-symmetry state by $(a_1\uparrow)^1(a_1\downarrow)^0(e\uparrow)^0(e\downarrow)^1(e\uparrow)^0(e\downarrow)^0(a_1\uparrow)^0(a_1\downarrow)^0$, but since the coupling involves different subsets of electrons on opposite metal centers, there are no associated states as such. However, we do recognize delocalized $S = 0'$ and $S = 1'$ states, $^1E'$ and $^3E'$, by the configurations $(a_1'\uparrow)^1(a_1'\downarrow)^0(e'\uparrow)^0(e'\downarrow)^1(e''\uparrow)^0(e''\downarrow)^0(a_2''\uparrow)^0(a_2''\downarrow)^0$ and $(a_1'\uparrow)^1(a_1'\downarrow)^0(e'\uparrow)^1(e'\downarrow)^0(e''\uparrow)^0(e''\downarrow)^0(a_2''\uparrow)^0(a_2''\downarrow)^0$, where the same electrons are aligned antiparallel and parallel, respectively (Scheme 1c). As written, the singlet configuration does not correspond to a pure spin state as it contributes to both $^1E'$ and $^3E'(M_S = 0)$ multiplets. Once again, using the sum method it is possible to express the energies of these two multiplets as a weighted sum of single-determinant energies as follows:

$$E(^3E') = E|a_1'^{+}e'_a{}^{+}| \tag{2a}$$

$$E(^1E') = 2E|a_1'^{+}e'_a{}^{-}| - E|a_1'^{+}e'_a{}^{+}| \tag{2b}$$

The potential energy curves for these two states and the broken-symmetry state are shown in Figure 3c, confirming that the delocalized $S = 1'$ spin-triplet again lies lower than the broken-symmetry state at all metal−metal separations, both having minima at approximately 3.25 Å. The global minimum for the asymmetric [$a_1 \times e$] coupling mode therefore corresponds to a spin-triplet state with $r$Ti−Ti = 3.28 Å.

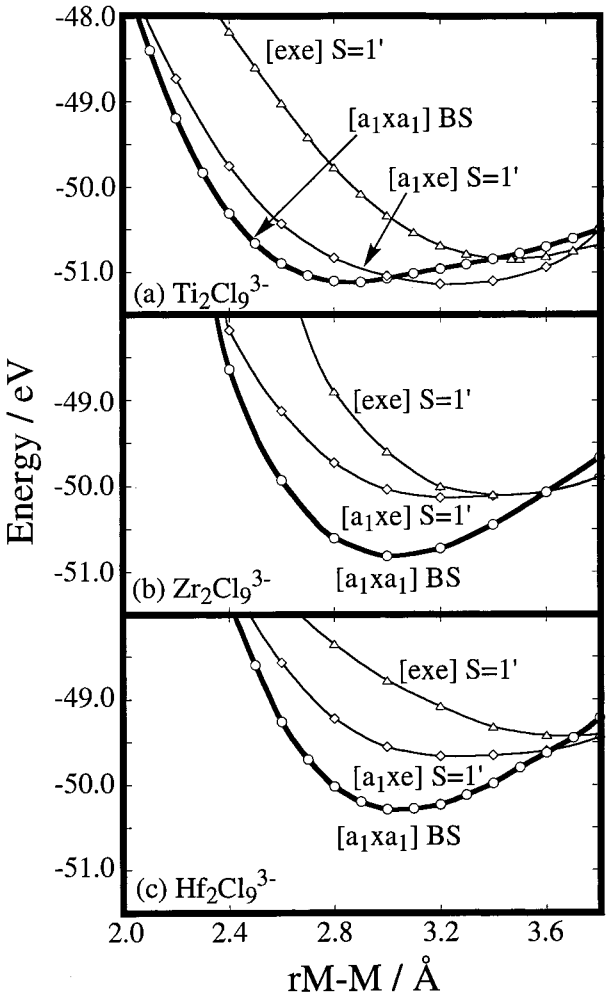


**Figure 4.** Potential energy curves for the broken-symmetry and $S = 1$ and $1'$ spin states for the [$a_1 \times a_1$], [e × e], and [$a_1 \times e$] coupling modes in $\{d^1d^1\}$ $M_2Cl_9^{3-}$ (M = Ti, Zr, Hf) complexes.

Having considered the three coupling modes in isolation, we are now in a position to examine which of the three represents the true global minimum, and therefore discuss the electronic properties of the $Ti_2Cl_9^{3-}$ ion. The earlier discussion revealed that the lowest energy state for the [$a_1 \times a_1$] mode was the broken-symmetry singlet, while for the [e × e] and [$a_1 \times e$] modes, the delocalized $S = 1'$ spin triplet states were most stable. The potential energy curves for these three states are brought together in Figure 4a. Some qualitative trends in optimized Ti−Ti separations become apparent when the three curves are compared. For [$a_1 \times a_1$], [$a_1 \times e$], and [e × e], the minimized values of $r$Ti−Ti are 2.87, 3.28, and 3.49 Å, consistent with the presence of 1, $^1/_2$, and 0 $\sigma$ bonds, respectively. The [$a_1 \times e$] triplet lies lower in energy than that from [e × e] because of the greater stability of the $\sigma$ bonding $a_1$ orbital. Thus, to determine the ground state of $Ti_2Cl_9^{3-}$, we simply need to evaluate the relative stabilities of two states: the broken-symmetry singlet arising from [$a_1 \times a_1$] and the triplet from [$a_1 \times e$]. Figure 4a indicates that the [$a_1 \times e$] $S = 1'$ state represents the global minimum, with an optimized Ti−Ti separation of 3.28 Å. We note, however, that the [$a_1 \times a_1$] singlet state lies only 0.02 eV higher than the triplet state, and given the

approximations inherent in the calculation, the singlet may represent the true ground state. Furthermore, given the proximity of these two levels energetically, environmental effects in the solid state may easily stabilize the singlet state over the triplet.

The $Ti_2X_9^{3-}$ (X = Cl, Br) systems have been the subject of several experimental and theoretical investigations mainly concerned with understanding the magnetic behavior of these complexes.[11] Solid-state magnetic susceptibility and inelastic neutron scattering studies[11e,h] indicate that in both complexes the dimer ground state is an orbitally nondegenerate spin-singlet level and that the closest excited states lie at least 400−500 $cm^{-1}$ to higher energy, consistent with strong antiferromagnetic behavior. In a detailed study by Leuenberger et al., the full orbitally degenerate exchange Hamiltonian was applied to the entire $^2T_2 \times {}^2T_2$ pair state manifold in order to fit the observed magnetic data.[11g] On the basis of their work, the separation of the ground $^1A_1'$ and excited $^3A_2''$ dimer states, arising from the occupation of the $a_1$ single-ion orbitals, corresponds to $|2J_{ab}|$ and was calculated to be approximately 700 $cm^{-1}$. From Table 1, the value of $|2J_{ab}|$, calculated using the optimized geometries of the singlet ground state and triplet excited-state associated with the $[a_1 \times a_1]$ coupling mode, is around 1450 $cm^{-1}$. Exchange coupling constants are typically overestimated by a factor of 2 by approximate density functional theory, and so our computational estimate is in agreement with the relatively strong antiferromagnetic coupling indicated by the experimental data. This description of the ground-state magnetic coupling in $Ti_2Cl_9^{3-}$ is also consistent with the detailed CASSCF/CASPT2 study of Ceulemans et al. who calculated a singlet−triplet gap of 650−800 $cm^{-1}$.[11j] They also showed that excited state multiplets belonging to the same coupling mode were energetically close, less than 200 $cm^{-1}$ apart, whereas multiplets belonging to different coupling modes were well separated energetically. This implies that our approach, where we are forced to average over spin-triplet multiplets arising from the $(e')^1(e'')^1$ configuration, is a reasonable approximation.

Although the heavier $d^1d^1$ analogues $Zr_2Cl_9^{3-}$ and $Hf_2Cl_9^{3-}$ do not exist, it is worthwhile examining these two complexes in order to investigate periodic trends in metal−metal bonding. The potential energy curves for the three coupling modes of $Zr_2Cl_9^{3-}$ and $Hf_2Cl_9^{3-}$ are shown for comparison in Figures 4b and 4c. In contrast to the titanium system, the minimum at *r*Zr−Zr = 3.01 Å for the $[a_1 \times a_1]$ singlet state now lies nearly 0.7 eV below both spin-triplet states, indicating that the metal-based electrons prefer to form a Zr−Zr $\sigma$ bond, and promotion of a single $a_1$ electron to the e orbital is an energetically costly process. On the basis of the calculated net spin density, complete delocalization of the $\sigma$ electrons occurs for *r*Zr−Zr < 3.6 Å representing a 0.6 Å increase relative to the titanium complex. The delocalization of the $\sigma$ electrons out to relatively large metal−metal distances is consistent with earlier *ab initio* calculations on other bimetallic zirconium(III) complexes which indicated substantial metal−metal overlap even at internuclear distances greater than 3.5 Å.[12] For the hafnium dimer, the stabilization of the $[a_1 \times a_1]$ singlet state relative to that of the spin triplet states is very similar to that of the zirconium dimer as is also the calculated metal−metal distance of 3.06 Å. The close correspondence of the potential energy curves and geometries in these two complexes highlights their similarity in electronic structure. We will analyze the periodic trends in these $d^1d^1$ complexes quantitatively later, but at this point we simply note the greater tendency toward delocalization of the metal-based electrons for complexes of the second and third transition series.

**$d^2d^2$ Complexes.** For $d^2d^2$ complexes, the electrons can reside in both the single-ion $a_1$ and e orbitals or alternatively, both electrons can occupy the e orbitals, giving rise to three different coupling modes, $[e^2 \times e^2]$, $[a_1e \times a_1e]$, and $[a_1e \times e^2]$. We follow the same procedure as for the $d^1d^1$ systems, analyzing each coupling mode in turn for a representative example from the first transition series, $V_2Cl_9^{3-}$, before bringing the three modes together to determine the nature of the global ground state. The symmetric $[e^2 \times e^2]$ coupling mode is the simplest of the three, because all orbitals are fully occupied, resulting in an orbitally nondegenerate $^3A_2$ single-ion ground state which gives rise to a spin-singlet, -triplet, and -quintet dimer levels of $^1A_1' + {}^3A_2'' + {}^5A_1'$ symmetry when coupling between the $\delta_\pi$ electrons is invoked. The broken-symmetry state is defined by the $(a_1\uparrow)^0(a_1\downarrow)^0(e\uparrow)^2(e\downarrow)^2(e\uparrow)^0(e\downarrow)^0(a_1\uparrow)^0(a_1\downarrow)^0$ configuration and the $S = 0$ and ferromagnetic $S = 2$ associated states by the $(a_1'\uparrow)^0(a_1'\downarrow)^0(e'\uparrow)^2(e'\downarrow)^2(e''\uparrow)^0(e''\downarrow)^0(a_2''\uparrow)^0(a_2''\downarrow)^0$ and $(a_1'\uparrow)^0(a_1'\downarrow)^0(e'\uparrow)^2(e'\downarrow)^0(e''\uparrow)^2(e''\downarrow)^0(a_2''\uparrow)^0(a_2''\downarrow)^0$ configurations, respectively (Scheme 2a). Potential energy curves for these three states are shown in Figure 5a, and the positions of the minima are summarized in Table 2. The curves follow the familiar pattern, with the broken-symmetry state lying close to $S = 2$ at large V−V separations (*r*V−V > 2.6 Å), and converging to $S = 0$ as the internuclear distance is decreased. Of the two associated states, $S = 2$ lies much lower than $S = 0$, and the global minimum in the broken-symmetry curve therefore occurs at 3.36 Å, coincident with that of the $S = 2$ associated state, indicating that the metal-based electrons are localized in the broken-symmetry state. From the calculated net spin density for the broken-symmetry state, complete delocalization of the metal-based $\delta_\pi$ electrons requires a very short metal−metal separation of 2.1 Å compared to 2.4 Å in the titanium dimer.

The symmetric $[a_1e \times a_1e]$ coupling mode, where both metals have an electron in each of the $a_1$ and e orbitals, is formally equivalent to the $[e \times e]$ mode of $d^1d^1$ complexes in that it gives rise to a half-filled e subshell. For this mode, the single-ion ground state is $^3E$ and coupling between the two metal centers results in spin-singlet, -triplet, and -quintet dimer levels in $D_{3h}$ symmetry. Once again the orbital degeneracy results in several dimer states of the same spin multiplicity and accordingly it will be necessary to use the sum method in order to determine the energies of the associated states. The broken-symmetry state is defined by $(a_1\uparrow)^1(a_1\downarrow)^1(e\uparrow)^1(e\downarrow)^1(e\uparrow)^0(e\downarrow)^0(a_1\uparrow)^0(a_1\downarrow)^0$, and the $S = 0$ and ferromagnetic $S = 2$ associated states by the full-symmetry $(a_1'\uparrow)^1(a_1'\downarrow)^1(e'\uparrow)^1(e'\downarrow)^1(e''\uparrow)^0(e''\downarrow)^0(a_2''\uparrow)^0(a_2''\downarrow)^0$ and $(a_1'\uparrow)^1(a_1'\downarrow)^0(e'\uparrow)^1(e'\downarrow)^0(e''\uparrow)^1(e''\downarrow)^0(a_2''\uparrow)^1(a_2''\downarrow)^0$ configurations, respectively (Scheme 2b). Analogous to the $[e \times e]$ mode of $d^1d^1$ complexes, the above singlet configuration does not correspond to a pure spin state as it contributes to $^3A_2'(M_S = 0) + {}^1E' + {}^1A_1'$ multiplets which arise from the $(a_1')^2(e')^2$ configuration. Using the sum method, the energies of these

(11) (a) Crough, P. C.; Fowles, G. W. A.; Walton, R. A. *J. Chem. Soc. A* **1967**, 517. (b) Saillant, R.; Wentworth, R. A. D. *Inorg. Chem.* **1968**, *7*, 1606. (c) Barraclough, C. R.; Gregson, A. K. *J. Chem. Soc., Faraday Trans.* **1972**, *177*, 2. (d) Kahn, O. *Mol. Phys.* **1975**, *29*, 1039. (e) Briat, B.; Kahn, O.; Morgenstern-Badarau, I.; Rivoal, C. *Inorg. Chem.* **1981**, *20*, 4193. (f) Drillon, M.; Georges, R. *Phys. Rev. B* **1982**, *26*, 3882. (g) Güdel, H. U.; Leuenberger, B. *Mol. Phys.* **1984**, *51*, 1. (h) Leuenberger, B.; Güdel, H. U.; Furrer, A. *Chem. Phys. Lett.* **1986**, *126*, 255. (i) Cotton, F. A.; Babaian-Kibala, E.; Falvello, L. R.; Shang, M. *Inorg. Chem.* **1990**, *29*, 2591. (j) Ceulemans, A. C.; Heylen, G. A.; Chibotaru, L. F.; Maes, T. L.; Pierloot, K.; Ribbing, C.; Vanquickenborne, L. G. *Inorg. Chim. Acta* **1996**, *251*, 15.

(12) Rohmer, M.-M.; Bénard, M. *Organometallics* **1991**, *10*, 157.

**Scheme 2**

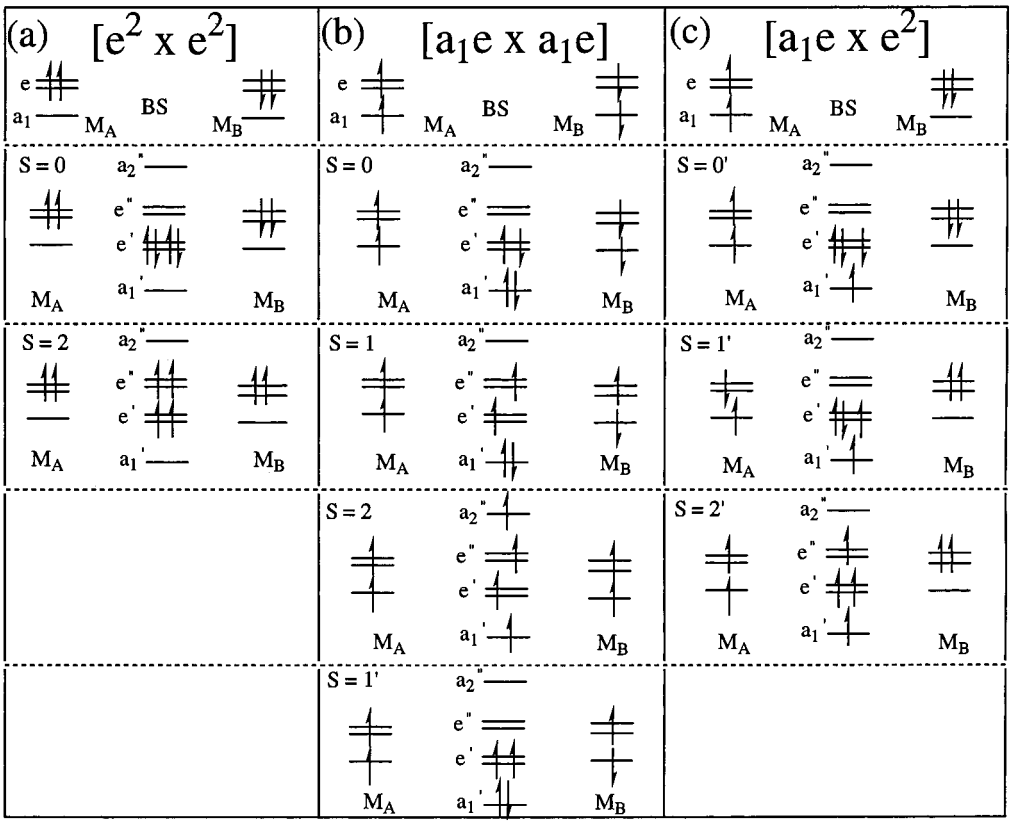


multiplets can be expressed in terms of the following single-determinant energies.

$$E(^3A_2') = E|a_1'^{+}a_1'^{-}e'_a{}^{+}e'_b{}^{+}| \quad (3a)$$

$$E(^1E') = 2E|a_1'^{+}a_1'^{-}e'_a{}^{+}e'_b{}^{-}| - E|a_1'^{+}a_1'^{-}e'_a{}^{+}e'_b{}^{+}| \quad (3b)$$

$$E(^1A_1') = 2E|a_1'^{+}a_1'^{-}e'_a{}^{+}e'_a{}^{-}| - 2E|a_1'^{+}a_1'^{-}e'_a{}^{+}e'_b{}^{-}| + E|a_1'^{+}a_1'^{-}e'_a{}^{+}e'_b{}^{+}| \quad (3c)$$

Again, the energies of these determinants are calculated in $C_{2v}$ symmetry in order to distinguish between the two components of the e′ orbitals. For the above quintet configuration $(a_1'\uparrow)^1(a_1'\downarrow)^0(e'\uparrow)^1(e'\downarrow)^0(e''\uparrow)^1(e''\downarrow)^0(a_2''\uparrow)^1(a_2''\downarrow)^0$ which spans $^5A_1' + {}^5A_2' + {}^5E'$ multiplets, only two single determinants of different energy can be found. Consequently, it is not possible to express the energy of these multiplets in terms of single-determinant energies.

In addition to the $S = 0$ and $S = 2$ associated states, intermediate associated states with $S = 1$, can also be defined by the $(a_1'\uparrow)^1(a_1'\downarrow)^1(e'\uparrow)^1(e'\downarrow)^0(e''\uparrow)^1(e''\downarrow)^0(a_2''\uparrow)^0(a_2''\downarrow)^0$ configuration corresponding to the decoupling of the $\delta_\pi$ electrons in isolation. This configuration gives rise to $^3A_1'' + {}^3A_2'' + {}^3E''$ multiplets but again only two single determinants of different energy can be found and consequently, it is not possible to obtain the energies of these multiplets uniquely. Although the calculated energies of both the $S = 1$ and $S = 2$ associated states correspond to weighted averages over multiplets of the same spin, this approximation does not affect the overall conclusion since it turns out that these states are not important in determining the global ground state in $V_2Cl_9^{3-}$.

Finally, from eq 3a, it is apparent that the degeneracy of the e′ dimer orbital again gives rise to an additional delocalized spin-triplet ($S = 1'$) state, $^3A_2'$, defined by the configuration $(a_1'\uparrow)^1(a_1'\downarrow)^1(e'\uparrow)^2(e'\downarrow)^0(e''\uparrow)^0(e''\downarrow)^0(a_2''\uparrow)^0(a_2''\downarrow)^0$ (Scheme 2b). For this state, the electrons are again coupled in parallel but occupy orthogonal components of the e′ dimer orbital, in contrast to the associated $S = 1$ states defined above where the same electrons occupy both e′ and e″ orbitals.

Potential energy curves for the broken-symmetry state (BS), the $^1E'$ spin-singlet ($S = 0$), average spin-triplet ($S = 1$) and average spin-quintet ($S = 2$) associated states, and the delocalized spin-triplet $S = 1'$ state are summarized in Figure 5b for the [$a_1e \times a_1e$] coupling mode. The potential energy curve for the $^1A_1'$ spin-singlet is not shown as it lies to higher energy. At long separations ($r$V−V > 3.4 Å) the broken-symmetry curve lies close to $S = 2$, indicating full localization, whereas at short separations $r$V−V < 2.2 Å, it converges with $S = 0$, indicating full delocalization. At intermediate separations, where 2.5 Å < $r$V−V < 2.9 Å, $S = 1$ lies lower than either $S = 0$ or $S = 2$, indicating that in this region, the ground state is best described as containing a V−V $\sigma$ bond, with the $\delta_\pi$ electrons only weakly coupled. The small vertical displacement of the $S = 1$ curve from the broken-symmetry curve in this region of $r$V−V is due to the incomplete coupling of the metal-based $\sigma$ electrons. As shown previously for the [$e^2 \times e^2$] mode, $S = 2$ is the lowest lying of all the associated states, and so the global minimum in the broken-symmetry state occurs at the localized limit corresponding to a long V−V separation of 3.22 Å. The potential energy curve for the $S = 1'$ state is observed to lie below the broken-symmetry curve at short V−V separations, where all metal-based electrons are delocalized, but as $r$V−V increases, this state then diverges to higher energy and follows the $S = 0$ associated state. As a result, the global minimum for the [$a_1e \times a_1e$] coupling mode of $V_2Cl_9^{3-}$ remains the localized broken-symmetry state.

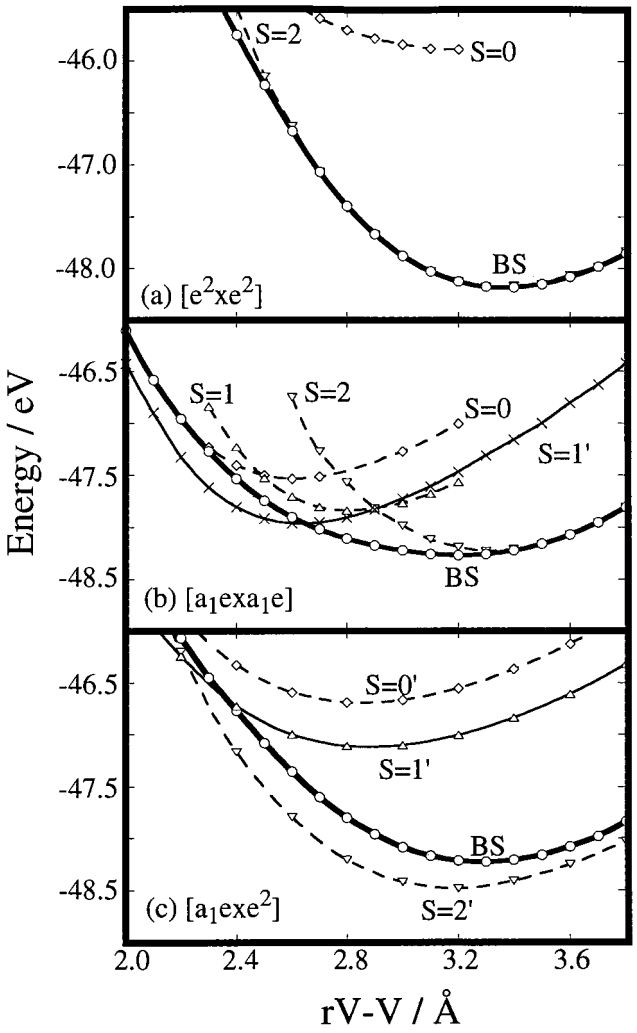


**Figure 5.** Potential energy curves for the broken-symmetry and $S = 0$, 1, 1′, 2, and 2′ spin states for the [$e^2 \times e^2$], [$a_1e \times a_1e$], and [$a_1e \times e^2$] coupling modes in $V_2Cl_9^{3-}$.

The behavior of the $S = 1'$ state contrasts markedly with the corresponding state for the [e × e] mode of $d^1d^1$ complexes, which lies below the broken-symmetry state at all metal−metal separations (Figure 3b), and it is instructive to consider the reasons for the different behavior. The delocalized and localized limits for the two $S = 1'$ states are shown in Schemes 1b and 2b, the delocalized limit is shown in the middle of the two isolated single-ion configurations on the left and right side of each figure which together correspond to the localized limit. For the $d^1d^1$ case, the $S = 1'$ state, corresponding to the $(e\uparrow)^1(e\uparrow)^1$ configuration at the localized limit, dissociates into two single ions, both with a spin-doublet ground state. However, at the dissociation limit of the $S = 1'$ state for the $d^2d^2$ configuration, $(a_1\uparrow)^1(a_1\downarrow)^1(e\uparrow)^1(e\uparrow)^1$, one single ion is in the triplet ground state, but the other is in an excited spin-singlet state, with the two electrons coupled antiparallel. As a result of this high energy localized asymptote, it is energetically favorable for the $S = 1'$ triplet to remain delocalized, even at long metal−metal separations, and hence the curve lies parallel to the $S = 0$ state, in which the electrons are delocalized, rather than the broken-symmetry state, where they are localized.

For the asymmetric [$a_1e \times e^2$] coupling mode, one metal ion has a $^3E$ ground state while the other has $^3A_2$. Coupling between the two metal centers again results in spin-singlet, -triplet, and -quintet dimer levels. We may define the broken-symmetry state by $(a_1\uparrow)^1(a_1\downarrow)^0(e\uparrow)^1(e\downarrow)^2(e\uparrow)^0(e\downarrow)^0(a_1\uparrow)^0(a_1\downarrow)^0$ but analogous to the $d^1d^1$ [$a_1 \times e$] asymmetric mode, it is not possible to define associated states as the coupling involves different subsets of electrons on opposite metal centers. However, once again delocalized spin-singlet ($S = 0'$) and spin-quintet ($S = 2'$) states, $^1E'$ and $^5E'$, where the same electrons are coupled antiparallel and parallel, respectively, can be defined by the configurations $(a_1'\uparrow)^1(a_1'\downarrow)^0(e'\uparrow)^1(e'\downarrow)^2(e''\uparrow)^0(e''\downarrow)^0(a_2''\uparrow)^0(a_2''\downarrow)^0$ and $(a_1'\uparrow)^1(a_1'\downarrow)^0(e'\uparrow)^2(e'\downarrow)^0(e''\uparrow)^1(e''\downarrow)^0(a_2''\uparrow)^0(a_2''\downarrow)^0$ (Scheme 2c). In addition, a delocalized spin-triplet ($S = 1'$) state, $^3E'$, can also be defined by the configuration $(a_1'\uparrow)^1(a_1'\downarrow)^0(e'\uparrow)^2(e'\downarrow)^1(e''\uparrow)^0(e''\downarrow)^0(a_2''\uparrow)^0(a_2''\downarrow)^0$.

Analogous to the [$a_1 \times e$] coupling mode in the $d^1d^1$ case, the singlet configuration does not correspond to a pure spin state as it contributes to both $^1E'$ and $^3E'(M_S = 0)$ multiplets. Using the sum method, the energies of these multiplets can be written in terms of the following single-determinant energies.

$$E(^3E') = E|a_1'^{+}e'_b{}^{+}e'_b{}^{-}e'_a{}^{+}| \quad (4a)$$

$$E(^1E') = 2E|a_1'^{+}e'_b{}^{+}e'_b{}^{-}e'_a{}^{-}| - E|a_1'^{+}e'_b{}^{+}e'_b{}^{-}e'_a{}^{+}| \quad (4b)$$

The potential energy curves for the broken-symmetry and delocalized $S = 0'$, 1′, and 2′ states are shown in Figure 5c. Just as in Figure 3c, the broken-symmetry and $S = 2'$ curves lie approximately parallel to each other, with minima in the region of 3.2−3.3 Å, and the high-spin state lies marginally

**Table 2.** Optimized Metal−Metal Separations (Å) and Ground State Energies (eV) for the Various Spin States of $d^2d^2$ $M_2X_9$ Complexes

| | | [$a_1e \times a_1e$] | | [$e^2 \times e^2$] | | [$a_1e \times e^2$] | |
|---|---|---|---|---|---|---|---|
| | | M−M/Å | E/eV | M−M/Å | E/eV | M−M/Å | E/eV |
| $V_2Cl_9^{3-}$ | BS | 3.23 | −48.266 | 3.36 | −48.184 | 3.29 | −48.229 |
| | $S = 0$ | 2.63 | −47.501 | 3.37 | −46.906 | | |
| | $S = 1$ | 2.81 | −47.860 | | | | |
| | $S = 2$ | 3.32 | −48.227 | 3.35 | −48.170 | | |
| | $S = 0'$ | | | | | 2.87 | −46.694 |
| | $S = 1'$ | 2.64 | −47.964 | | | 2.89 | −47.120 |
| | $S = 2'$ | | | | | 3.18 | −48.483 |
| $Nb_2Cl_9^{3-}$ | BS | 2.68 | −51.022 | 3.62 | −50.058 | 3.41 | −50.167 |
| | $S = 0$ | 2.68 | −51.009 | 3.63 | −49.599 | | |
| | $S = 1$ | 2.92 | −50.773 | | | | |
| | $S = 2$ | 3.55 | −49.989 | 3.60 | −49.972 | | |
| | $S = 0'$ | | | | | 2.73 | −49.764 |
| | $S = 1'$ | 2.69 | −51.285 | | | 2.74 | −50.029 |
| | $S = 2'$ | | | | | 3.32 | −50.498 |
| $Ta_2Cl_9^{3-}$ | BS | 2.74 | −50.678 | 3.67 | −49.508 | 3.43 | −49.676 |
| | $S = 0$ | 2.73 | −50.645 | 3.71 | −49.119 | | |
| | $S = 1$ | 2.97 | −50.369 | | | | |
| | $S = 2$ | 3.61 | −49.457 | 3.67 | −49.415 | | |
| | $S = 0'$ | | | | | 2.77 | −49.426 |
| | $S = 1'$ | 2.75 | −50.923 | | | 2.77 | −49.695 |
| | $S = 2'$ | | | | | 3.35 | −50.010 |
| $Nb_2Br_9^{3-}$ | BS | 2.74 | −46.355 | 3.75 | −45.522 | 3.58 | −45.622 |
| | $S = 0$ | 2.74 | −46.355 | 3.77 | −44.993 | | |
| | $S = 1$ | 3.01 | −46.133 | | | | |
| | $S = 2$ | 3.67 | −45.482 | 3.74 | −45.458 | | |
| | $S = 0'$ | | | | | 2.78 | −45.533 |
| | $S = 1'$ | 2.76 | −46.603 | | | 2.79 | −45.455 |
| | $S = 2'$ | | | | | 3.49 | −45.932 |
| $Nb_2I_9^{3-}$ | BS | 2.80 | −40.924 | 3.99 | −40.294 | 3.78 | −40.379 |
| | $S = 0$ | 2.80 | −40.918 | 4.00 | −39.731 | | |
| | $S = 1$ | 3.11 | −40.772 | | | | |
| | $S = 2$ | 3.85 | −40.291 | 3.87 | −40.245 | | |
| | $S = 0'$ | | | | | 2.83 | −39.923 |
| | $S = 1'$ | 2.81 | −41.165 | | | 2.85 | −40.140 |
| | $S = 2'$ | | | | | 3.66 | −40.653 |

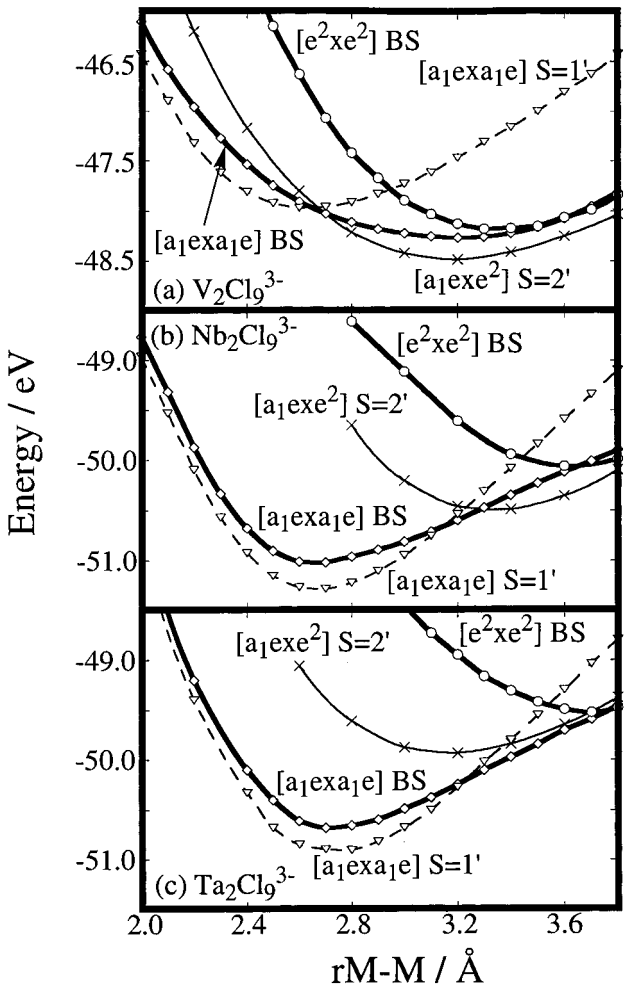


**Figure 6.** Potential energy curves for the broken-symmetry and $S = 1'$ and $2'$ spin states for the $[e^2 \times e^2]$, $[a_1e \times a_1e]$, and $[a_1e \times e^2]$ coupling modes in $\{d^2d^2\}$ $M_2Cl_9^{3-}$ (M = V, Nb, Ta) complexes.

lower at all metal−metal separations. Thus, the global minimum arising from the $[a_1e \times e^2]$ coupling mode corresponds to the spin-quintet state.

Collecting together all the candidates for the global minimum for the $d^2d^2$ complexes, we now have four possibilities to consider. For the $[e^2 \times e^2]$ mode, the broken-symmetry singlet lies lowest, while for the asymmetric $[a_1e \times e^2]$ mode, the spin quintet, $S = 2'$, lies lowest. For $[a_1e \times a_1e]$, there are two possibilities − the delocalized triplet $S = 1'$ lies lowest at short separations, while the broken-symmetry state lies lowest at longer *r*M−M. All four states are collected together in Figure 6a. At short V−V separations, the $S = 1'$ state arising from the $[a_1e \times a_1e]$ coupling mode, where a V−V $\sigma$ bond is present, lies lower than the broken-symmetry state from $[e^2 \times e^2]$ because of the presence of a $\sigma$ bond in the former. As the metal−metal separation is increased, this $S = 1'$ state moves to higher energy, and over a narrow range around 2.7 Å, the $[a_1e \times a_1e]$ broken-symmetry singlet becomes the ground state. At longer separations, the promotion of an electron from $a_1$ to e becomes more favorable, and the $[a_1e \times e^2]$ $S = 2'$ spin-quintet state becomes the ground state. For $V_2Cl_9^{3-}$, this spin-quintet state corresponds to the global minimum, lying approximately 0.2 eV lower than any of the other states, consistent with the ferromagnetically coupled ($J_{ab} = 11$ cm$^{-1}$) ground state reported by Güdel and co-workers.[13] The optimized V−V separation of 3.18 Å, is also in excellent agreement with the reported value of 3.16 Å for $Cs_3V_2Cl_9$.

Potential energy curves for the corresponding states for $Nb_2Cl_9^{3-}$ are illustrated in Figure 6b, and show several distinct differences in comparison to $V_2Cl_9^{3-}$. The minimum in the broken-symmetry state arising from the $[a_1e \times a_1e]$ coupling mode occurs at a much shorter metal−metal separation, and is coincident with that for the $S = 0$ associated state rather than $S = 2$ (Table 2), indicating that the metal-based electrons are fully delocalized. The $S = 1'$ triplet state arising from the same coupling mode again follows the $S = 0$ curve, with the result that it now represents the global minimum for $Nb_2Cl_9^{3-}$, lying some 0.8 eV below the $[a_1e \times e^2]$ $S = 2'$ quintet. The minimum is calculated to have a Nb−Nb separation of 2.69 Å, in excellent accord with experimental estimates of 2.68 Å.[14a] The ground-state structure of $Nb_2Cl_9^{3-}$ (short *r*Nb−Nb, spin-triplet) which corresponds to a Nb−Nb double bond, contrasts markedly with that of its lighter vanadium analogue (long *r*V−V, spin-quintet), and the periodic trends can again be accounted for simply in terms of the greater radial extension of the 4d orbitals, which stabilizes states where a $\sigma$ bond is present ($[a_1e \times a_1e]$ broken-symmetry and $S = 1'$) relative to the others.

In contrast to the accurate estimation of the Nb−Nb separation in $Nb_2Cl_9^{3-}$, the spin-triplet ground state is apparently at odds with the reported magnetic moment, which is rather lower than that anticipated for a complex with two unpaired electrons.[14b,c] In contrast, the magnetic moments of the bromide and iodide analogues are much higher than the chloride, consistent with the bonding scheme outlined above.[14a,b] The corresponding curves for the bromide and iodide complexes (not shown) reveal no significant qualitative or quantitative differences compared to the chloride, with the $S = 1'$ triplet lying approximately 0.2 eV below the singlet in each case (see Table 2). Thus, the density functional calculations reported here provide no explanation for the apparently anomalous magnetic properties of $Nb_2Cl_9^{3-}$. Cotton and co-workers[15] have reported Xα-SW and *ab initio* calculations on $Nb_2Cl_9^{3-}$, and also found the triplet to lie lowest.

For comparative purposes, we have also undertaken calculations on the structurally uncharacterized tantalum complex $Ta_2Cl_9^{3-}$. The energy minima and optimized internuclear separations for the states associated with the three different coupling modes are given in Table 2 and the relevant potential energy curves are shown in Figure 6c. Not unexpectedly, the same mode of coupling is predicted for this system as for $Nb_2Cl_9^{3-}$ with the $S = 1'$ triplet state stabilized by over 0.2 eV relative to the other states. As was found for the niobium complex, the optimized Ta−Ta distance of 2.75 Å corresponds to complete delocalization of both the $\sigma$ and $\delta_\pi$ electrons and thus a Ta−Ta double bond.

**Periodic Trends across a Transition Series.** During the preceding discussions we have emphasized periodic trends down a triad, a subject which we analyzed in some detail in recent publications.[5b,c] Having examined the $d^1d^1$, $d^2d^2$, and $d^3d^3$ systems, we are now in a position to consider trends in metal−metal bonding across a period. The potential energy curves illustrated in Figures 4 and 6 indicate that metal−metal bonding tends to be weaker in the $d^2d^2$ complexes than in their $d^1d^1$ counterparts, despite the increase in formal bond order from 1 to 2. This is best exemplified by considering the broken-symmetry states in which the $a_1$ orbitals are occupied, corre-

(13) Leuenberger, B.; Briat, B.; Canit, J. C.; Furrer, A.; Fischer, P.; Güdel, H. U. *Inorg. Chem.* **1986**, *25*, 2930.
(14) (a) Broll, A.; von Schnering, H. G.; Schäfer, H. *J. Less Common. Met.* **1970**, *22*, 243. (b) Maas, E. T., Jr.; McCarley, R. E. *Inorg. Chem.* **1973**, *12*, 1096. (c) Cotton, F. A.; Feng, X.; Gütlich, P.; Kohlhaas, T.; Lu, J.; Shang, M. *Inorg. Chem.* **1994**, *33*, 3055.
(15) Cotton, F. A.; Feng, X. *Int. J. Quantum Chem.* **1996**, *58*, 671.

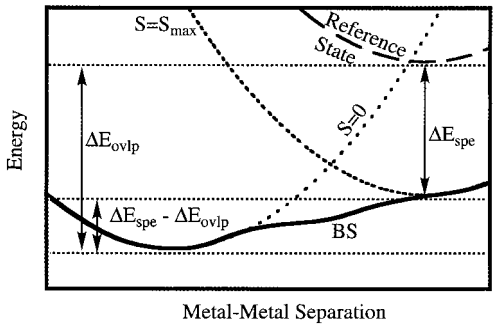


**Figure 7.** Schematic representation of the terms $\Delta E_{spe}$ and $\Delta E_{ovlp}$ in relation to the $S = 0$, $S_{max}$, and reference states of $d^nd^n$ ($n = 1-3$) dimers.

sponding to the $[a_1 \times a_1]$ and $[a_1e \times a_1e]$ coupling modes for $d^1d^1$ and $d^2d^2$ configurations, respectively. For $Ti_2Cl_9^{3-}$, the electrons are delocalized (Figure 3a), while in the vanadium analogue, they are localized (Figure 5b). In the $d^3d^3$ chromium system, $Cr_2Cl_9^{3-}$, described previously, the electrons are also completely localized. Thus it appears that the tendency of metal-based electrons to delocalize, and therefore their ability to participate in a metal−metal bond, varies inversely with the formal bond order.

In a previous paper,[5b] we quantified the driving force for electron delocalization in $d^3d^3$ complexes by considering the relative energies of the two associated states, $S = 0$ and $S_{max} = 3$ (Figure 7). The broken-symmetry curve follows the path of lowest energy between these two states, and so the position of the broken-symmetry minimum, and therefore the nature of the metal−metal bonding, is determined simply by the relative energies of the $S = 0$ and $S = 3$ states. Furthermore, we can equate the depth of the $S = 0$ curve, where the electrons are delocalized and the bonding molecular orbitals are occupied, with the stabilizing effects of orbital overlap. In contrast, the depth of the $S = 3$ curve, where there is no metal−metal bond but an excess of 3 spin-up electrons per metal center, can be equated with the stabilizing influence of spin polarization on the metals. By employing a suitable reference state defined by the configuration $[(a_1'\uparrow)^{1/2}(a_1'\downarrow)^{1/2}(e'\uparrow)^1(e'\downarrow)^1(e''\uparrow)^1(e''\downarrow)^1(a_2''\uparrow)^{1/2}$-$(a_2''\downarrow)^{1/2}]$, where neither metal−metal bonding nor spin polarization are present, we can obtain independent estimates of the energetic contributions of orbital overlap ($\Delta E_{ovlp}$) and spin polarization ($\Delta E_{spe}$) for the dimer. Thus, high values of $\Delta E_{ovlp}$ indicate a stable $S = 0$ state, favoring delocalization of electrons, while high values of $\Delta E_{spe}$ indicate a stable $S = 3$ state, favoring localization. The difference between the two terms, $\Delta E_{spe} - \Delta E_{ovlp}$, defines the position of the localized/delocalized equilibrium. The reader is referred to ref 5b for a full discussion of these concepts.

Having described in detail the potential energy curves of the $d^1d^1$ and $d^2d^2$ systems, we are now able to extend this form of analysis to explore trends across a transition series as well as down a group. In each case, we consider the broken-symmetry state with the $a_1$ orbitals occupied, i.e., $[a_1 \times a_1]$, $[a_1e \times a_1e]$ and $[a_1e^2 \times a_1e^2]$ for $d^1d^1$, $d^2d^2$ and $d^3d^3$ systems, respectively. In Figure 7, the $\Delta E_{ovlp}$ term is identified with the separation between the reference and $S = 0$ associated states, while $\Delta E_{spe}$ is identified with the separation between the reference and the appropriate $S = S_{max}$ state where $S_{max} = 1$, 2, and 3 for $d^1d^1$, $d^2d^2$, and $d^3d^3$ systems, respectively. By analogy with the $d^3d^3$ case, the reference states are defined by the configurations $[(a_1'\uparrow)^{1/6}(a_1'\downarrow)^{1/6}(e'\uparrow)^{1/3}(e'\downarrow)^{1/3}(e''\uparrow)^{1/3}(e''\downarrow)^{1/3}(a_2''\uparrow)^{1/6}(a_2''\downarrow)^{1/6}]$ for $d^1d^1$ and $[(a_1'\uparrow)^{1/3}(a_1'\downarrow)^{1/3}(e'\uparrow)^{2/3}(e'\downarrow)^{2/3}(e''\uparrow)^{2/3}(e''\downarrow)^{2/3}(a_2''\uparrow)^{1/3}(a_2''\downarrow)^{1/3}]$ for $d^2d^2$. The two terms, $\Delta E_{ovlp}$ and $\Delta E_{spe}$, along with their difference, are summarized in Table 3 for the first-, second-, and third-row nonachlorides, $M_2Cl_9^{3-}$, M = Ti, V, Cr, Zr, Nb, Mo, Hf, Ta, W. The single-ion spin polarization energies, defined as the difference between spin-restricted $[(t_{2g}\uparrow)^{n/2}(t_{2g}\downarrow)^{n/2}]$ and spin-unrestricted $[(t_{2g}\uparrow)^n(t_{2g}\downarrow)^0]$ ($n = 1, 2, 3$) energies of the metal hexachlorides, $MCl_6^{3-}$, are also included for comparison.

**Table 3.** Overlap and Spin Polarization Energies (eV) for $MCl_6^{3-}$ and $M_2Cl_9^{3-}$ Complexes (See Text for Definition of Terms)

| | | $\Delta E_{ovlp}$ | $\Delta E_{spe}$ | $\Delta E_{spe} - \Delta E_{ovlp}$ | single-ion SPE | |
|---|---|---|---|---|---|---|
| | $[Ti_2Cl_9]^{3-}$ | 0.659 | 0.299 | −0.360 | $[TiCl_6]^{3-}$ | 0.199 |
| $[a_1 \times a_1]$ | $[Zr_2Cl_9]^{3-}$ | 1.511 | 0.242 | −1.269 | $[ZrCl_6]^{3-}$ | 0.136 |
| | $[Hf_2Cl_9]^{3-}$ | 1.474 | 0.167 | −1.307 | $[HfCl_6]^{3-}$ | 0.130 |
| | $[V_2Cl_9]^{3-}$ | 0.860 | 1.545 | +0.685 | $[VCl_6]^{3-}$ | 0.817 |
| $[a_1e \times a_1e]$ | $[Nb_2Cl_9]^{3-}$ | 2.036 | 1.003 | −1.033 | $[NbCl_6]^{3-}$ | 0.532 |
| | $[Ta_2Cl_9]^{3-}$ | 2.141 | 0.922 | −1.219 | $[TaCl_6]^{3-}$ | 0.493 |
| | $[Cr_2Cl_9]^{3-}$ | 1.017 | 3.547 | +2.530 | $[CrCl_6]^{3-}$ | 1.859 |
| $[a_1e^2 \times a_1e^2]$ | $[Mo_2Cl_9]^{3-}$ | 2.882 | 2.192 | −0.690 | $[MoCl_6]^{3-}$ | 1.144 |
| | $[W_2Cl_9]^{3-}$ | 3.096 | 1.997 | −1.099 | $[WCl_6]^{3-}$ | 1.034 |

The $\Delta E_{ovlp}$ term reflects the change in formal bond order from 1 to 3 across the series, increasing steadily from $d^1d^1$ to $d^3d^3$. In the first transition series, the $\sigma$ bond contributes approximately 0.65 eV to the stability of the system, while each additional $\delta_\pi$ component contributes a further 0.2 eV. In the second and third transition series, where the orbitals are rather more diffuse, the $\sigma$ bond is stronger corresponding to approximately 1.5 eV and the additional $\delta_\pi$ bonds contribute between 0.5 and 1.0 eV. Thus, on the basis of the contribution of orbital overlap alone, we would anticipate stronger bonding in $d^3d^3$ complexes. In each system, the $\Delta E_{spe}$ term is approximately equal to twice the single-ion spin polarization energy, confirming it is determined essentially by the sum of the properties of the isolated single ions. The decrease in $\Delta E_{spe}$ down a triad, described previously for the chromium triad, persists in the $d^1d^1$ and $d^2d^2$ systems, and is simply due to the greater average interelectron separation in the larger 4d and 5d orbitals.

Moving across a period, the number of electrons per metal center increases from 1 to 3, and this is accompanied by a dramatic increase in single-ion spin polarization energy, from 0.199 ($Ti^{3+}$) to 0.817 ($V^{3+}$) and then 1.859 ($Cr^{3+}$). The spin polarization (or exchange) energy is dependent upon the number of pairs of like spin electrons, $n!/2$, and so, considering only the valence d electrons, should vary in the ratio 0:1:3 for $d^1$, $d^2$, and $d^3$ systems. The single-ion spin polarization energies for $MCl_6^{3-}$ (and therefore $\Delta E_{spe}$ for the dimers) follow this pattern approximately, with the separation between $d^1$ and $d^2$ roughly half that between $d^2$ and $d^3$. Thus, while both $\Delta E_{ovlp}$ (favoring electron delocalization) and $\Delta E_{spe}$ (favoring localization) increase with electron count, the functional dependence on n is very different. $\Delta E_{ovlp}$ varies approximately linearly with n, while $\Delta E_{spe}$ increases far more rapidly, approximately as n!. For the $d^1d^1$ systems, $\Delta E_{ovlp}$ is always greater than $\Delta E_{spe}$, giving negative values of $\Delta E_{spe} - \Delta E_{ovlp}$, and hence a delocalized ground state, but as further electrons are added, the rapid increase in $\Delta E_{spe}$ dominates changes in $\Delta E_{ovlp}$. The result is that $\Delta E_{spe} - \Delta E_{ovlp}$ becomes less negative, and for complexes of the first transition series, where the small 3d orbitals give rise to high $\Delta E_{spe}$ and low $\Delta E_{ovlp}$, becomes positive, giving rise to localized broken-symmetry states for both $V_2Cl_9^{3-}$ and $Cr_2Cl_9^{3-}$. Similar trends are present for the complexes of the second and third transition series, but in these cases the larger $\Delta E_{ovlp}$ and smaller $\Delta E_{spe}$ associated with the more diffuse 4d and 5d orbitals means that $\Delta E_{spe} - \Delta E_{ovlp}$ remains negative, even for the $d^3d^3$ complexes, $Mo_2Cl_9^{3-}$ and $W_2Cl_9^{3-}$.

The above discussion indicates that we should expect the tendency for electrons to delocalize in a dimer to decrease as the number of unpaired electrons on each metal center increases. Thus moving across a period, the most localized complexes will correspond to those with $d^3$ ($Cr^{3+}$, $Mn^{4+}$) and high-spin $d^5$ ($Mn^{2+}$, $Fe^{3+}$) configurations, while those with only one unpaired electron, $d^1$ ($Ti^{3+}$) or low-spin $d^5$ ($Ru^{3+}$), will favor delocalized ground states, even at relatively long metal−metal separations. Thus far we have dealt only with homonuclear $d^1d^1$, $d^2d^2$, and $d^3d^3$ dimers, but in a future study we intend to investigate heteronuclear $d^nd^n$ and $d^nd^m$ ($n$, $m = 1-3$) complexes, both even- and odd-electron systems. It is also worthwhile mentioning that this type of analysis is also applicable in the study of low-spin/high-spin equilibria in $d^nd^n$ ($n = 4-6$) dimers. We are currently working on this problem in relation to $d^5d^5$ dimers of the Fe triad.

## Conclusion

In this study, approximate density functional theory has been used to generate potential energy curves for the broken-symmetry and associated spin states of $d^1d^1$ and $d^2d^2$ face-shared $M_2X_9^{3-}$ dimers of Ti, Zr, Hf ($d^1d^1$) and V, Nb, Ta ($d^2d^2$) in order to investigate their electronic and geometric structures and periodic trends in metal−metal bonding. For these bimetallic systems the mode of coupling and extent of metal−metal bonding, and as a consequence the ground-state geometry, is dependent on the occupation of the trigonal $a_1$ and e orbitals on each metal center. For both systems three distinct coupling modes can be recognized corresponding to $[a_1 \times a_1]$, $[e \times e]$, and $[a_1 \times e]$ for $d^1d^1$ complexes and $[a_1e \times a_1e]$, $[e^2 \times e^2]$, and $[a_1e \times e^2]$ for $d^2d^2$ complexes. For the symmetric coupling modes, a broken-symmetry state can be identified along with $S = 0, 1$ ($d^1d^1$) and $S = 0, 1, 2$ ($d^2d^2$) associated states where the weakly coupled subsets of electrons are aligned in parallel. Additional spin-triplet states, denoted $S = 1'$, also arise in the delocalized limit for both the $[e \times e]$ $d^1d^1$ and $[a_1e \times a_1e]$ $d^2d^2$ modes where two electrons are aligned parallel in orthogonal components of the $\delta_\pi$ (e′) bonding orbital. For the asymmetric modes $[a_1 \times e]$ and $[a_1e \times e^2]$, a broken-symmetry state is also identified but since the coupling involves different subsets of electrons on opposite centers, no associated states are defined. However, for these modes $S = 0', 1'$ ($d^1d^1$) and $S = 0', 1', 2'$ ($d^2d^2$) delocalized states are possible.

For the $d^1d^1$ complexes $Ti_2Cl_9^{3-}$, $Zr_2Cl_9^{3-}$, and $Hf_2Cl_9^{3-}$, the ground-state geometry is determined by the relative energies of the $[a_1 \times a_1]$ broken-symmetry state and the spin-triplet $S = 1'$ states associated with the $[e \times e]$ and $[a_1 \times e]$ coupling modes. For $Ti_2Cl_9^{3-}$, the $[a_1 \times a_1]$ broken-symmetry and $[a_1 \times e]$ spin-triplet ($S = 1'$) states are of similar energy and therefore the resulting geometry is likely to be sensitive to solid-state packing effects. The $[a_1 \times a_1]$ broken-symmetry optimized structure, however, corresponds to significant delocalization of the metal-based electrons and effectively a Ti−Ti $\sigma$ bond, nicely rationalizing the strong antiferromagnetic coupling reported for $Cs_3Ti_2Cl_9$. For both $Zr_2Cl_9^{3-}$ and $Hf_2Cl_9^{3-}$, the $[a_1 \times a_1]$ broken-symmetry state is significantly stabilized relative to all other states and thus the ground-state geometry of these complexes corresponds to complete delocalization of the metal-based electrons in a metal−metal $\sigma$ bond. In both these complexes, the metal-based electrons remain completely delocalized even out to internuclear distances of 3.6 Å.

In the case of the $d^2d^2$ complexes $V_2Cl_9^{3-}$, $Nb_2Cl_9^{3-}$, and $Ta_2Cl_9^{3-}$, the ground-state geometry is determined by the relative energies of the broken-symmetry and spin-triplet $S = 1'$ states associated with the $[a_1e \times a_1e]$ coupling mode and the spin-quintet $S = 2'$ state of the $[a_1e \times e^2]$ mode. At shorter internuclear separations the $[a_1e \times a_1e]$ $S = 1'$ state is most stable whereas at longer separations the ground state corresponds to the $[a_1e \times e^2]$ spin-quintet. For $V_2Cl_9^{3-}$, the global minimum is found to be the ferromagnetic $[a_1e \times e^2]$ $S = 2'$ state giving rise to a relatively long V−V separation of 3.18 Å, consistent with the known structure and reported weak ferromagnetic behavior of $Cs_3V_2Cl_9$. For $Nb_2X_9^{3-}$ (X = Cl, Br, I) and $Ta_2Cl_9^{3-}$, the $[a_1e \times a_1e]$ $S = 1'$ state, corresponding to the complete delocalization of the metal-based $\sigma$ and $\delta_\pi$ electrons in a metal−metal double bond, is found to be the global minimum and consequently relatively short internuclear distances result. The optimized metal−metal separation of 2.69 Å for $Nb_2Cl_9^{3-}$ is in excellent agreement with experiment. Although neither of the three broken-symmetry states corresponds to the global minimum for these complexes, the optimized geometry for the $[a_1e \times a_1e]$ broken-symmetry state is in all cases very close to that of the global minimum.

The periodic trends in metal−metal bonding in these complexes can be rationalized in terms of the energetic contributions of orbital overlap ($\Delta E_{ovlp}$) favoring delocalization and spin polarization ($\Delta E_{spe}$) favoring localization, the difference between the two terms $\Delta E_{spe} - \Delta E_{ovlp}$ determining the tendency of the metal-based electrons to delocalize. Down a triad $\Delta E_{ovlp}$ increases due to the greater radial dilation of the 4d and 5d orbitals. Across a period $\Delta E_{ovlp}$ also increases, reflecting the change in formal bond order from 1 to 3. The spin polarization term $\Delta E_{spe}$ decreases down a triad, a consequence of the greater dilation of the 4d and 5d orbitals which reduces the average interelectron separation, whereas across a series this term increases dramatically due to the progressive increment in d electrons and contraction in the d orbitals arising from the increased nuclear charge. For the $d^1d^1$ systems, $\Delta E_{ovlp}$ is always greater than $\Delta E_{spe}$ and therefore delocalized ground states result for all complexes of the titanium triad. Moving across the first transition series however, the dramatic increase in $\Delta E_{spe}$ dominates the increase in $\Delta E_{ovlp}$ with the result that the $d^2d^2$ and $d^3d^3$ complexes $V_2Cl_9^{3-}$ and $Cr_2Cl_9^{3-}$ have localized ground states. Similar trends are found for the second and third transition series but the much larger $\Delta E_{ovlp}$ term ensures that these complexes remain delocalized, even for the $d^3d^3$ complex $Mo_2Cl_9^{3-}$.

**Acknowledgment.** We gratefully acknowledge the Australian Research Council (ARC) for financial support and the EPSRC (U.K.) for a scholarship to T.L. We also acknowledge the helpful comments from the reviewers of this paper.

IC971511Y